Development 140, 4246-4255 (2013) doi:10.1242/dev.093625

Gprk2 adjusts Fog signaling to organize cell movements in *Drosophila* gastrulation

Naoyuki Fuse[1,2,3,*], Fengwei Yu[4] and Susumu Hirose[1,2]

SUMMARY

Gastrulation of *Drosophila melanogaster* proceeds through sequential cell movements: ventral mesodermal (VM) cells are induced by secreted Fog protein to constrict their apical surfaces to form the ventral furrow, and subsequently lateral mesodermal (LM) cells involute toward the furrow. How these cell movements are organized remains elusive. Here, we observed that LM cells extended apical protrusions and then underwent accelerated involution movement, confirming that VM and LM cells display distinct cell morphologies and movements. In a mutant for the GPCR kinase Gprk2, apical constriction was expanded to all mesodermal cells and the involution movement was abolished. In addition, the mesodermal cells halted apical constriction prematurely in accordance with the aberrant accumulation of Myosin II. Epistasis analyses revealed that the *Gprk2* mutant phenotypes were dependent on the *fog* gene. Overexpression of Gprk2 suppressed the effects of excess Cta, a downstream component of Fog signaling. Based on these findings, we propose that Gprk2 attenuates and tunes Fog-Cta signaling to prevent apical constriction in LM cells and to support appropriate apical constriction in VM cells. Thus, the two distinct cell movements in mesoderm invagination are not predetermined, but rather are organized by the adjustment of cell signaling.

KEY WORDS: *Drosophila*, Gprk2, Gastrulation

INTRODUCTION

During morphogenetic movements in the course of development, cells dynamically change their shapes and positions (Leptin, 2005; Solnica-Krezel and Sepich, 2012). These cell movements are spatially and temporally organized for shaping tissues and embryos into their correct forms. Forces driving cell movements are generated by cytoskeletal filaments and motor proteins, such as actin filaments and myosin motors (Jacinto et al., 2002; Lecuit and Lenne, 2007; Martin, 2010). Cell-cell adhesions and intercellular signals regulate force generators in each cell and are thought to organize cell movements in a spatiotemporal manner. However, the cellular mechanics and signals governing cell movements at the tissue level are not fully understood.

Gastrulation of *Drosophila melanogaster* is an ideal system for studying morphogenetic movement, as cell movements occur in spatially distinct regions on a precise schedule (Costa et al., 1993). A cellular blastoderm embryo (3 hours after egg laying) consists of ~6000 epithelial cells surrounding the outer cortex. About 1000 cells on the ventral side acquire mesodermal cell fate by means of the activity of Twist (Twi) and Snail transcription factors, and these cells then invaginate into the embryo. During mesoderm invagination, ventral mesodermal (VM) cells, which typically expand to a 12-cell width along the dorsoventral axis, constrict their apical cell surfaces. Consequently, the epithelial sheet bends and a ventral furrow is formed along the anteroposterior axis (see Fig. 1A, Fig. 2A). A recent report proposed that the constrictive force operates isotropically in each VM cell, but that a tissue-level tension along the longer anteroposterior axis restricts the apical constriction anisotropically to the dorsoventral axis (Martin et al., 2010). Apical constriction is not the only cell movement during mesoderm invagination. Lateral mesodermal (LM) cells, which are located on the sides of VM cells (typically a three-cell width on each side), do not undergo apical constriction, but involute toward the ventral furrow (see Fig. 3A,C). Finally, left and right LM cells meet at the midline and close the furrow (see Fig. 3E). These cell movements proceed sequentially and mesoderm invagination is completed within 15 minutes. The movement of LM cells has not been characterized in detail, and it has also remained unclear how the VM/LM area is defined in mesodermal cells (Leptin and Roth, 1994).

Previous studies have revealed molecular mechanisms regulating the apical constriction of VM cells (Lecuit and Lenne, 2007; Martin, 2010). According to a current model, the secreted signaling protein Folded gastrulation (Fog), which is expressed in a Twi-dependent manner, induces the apical constriction (Costa et al., 1994; Morize et al., 1998). The Fog receptor remains unknown, but is expected to be a G protein-coupled receptor (GPCR) because a heterotrimeric G protein Gα subunit [Concertina (Cta)] acts in the downstream signaling (Parks and Wieschaus, 1991). Fog signaling stimulates the apical localization of Myosin II protein, which generates a force that constricts the cell surface (Dawes-Hoang et al., 2005). In parallel with Fog signaling, other pathways coordinately regulate the actomyosin network to induce apical constriction. The transmembrane protein T48, which is another target of Twi, regulates the localization of myosin motors through direct binding with RhoGEF2 (Kölsch et al., 2007). Abelson kinase together with RhoGEF2 organizes actin filaments at the apical cell surface (Barrett et al., 1997; Fox and Peifer, 2007). These parallel pathways explain the incomplete progression of apical constriction in the absence of one pathway, as seen in *fog* mutant embryos (Sweeton et al., 1991; Costa et al., 1994; Kölsch et al., 2007).

[1]Department of Developmental Genetics, National Institute of Genetics, Yata 1111, Mishima 411-8540, Japan. [2]Graduate University for Advanced Studies, Yata 1111, Mishima 411-8540, Japan. [3]Laboratory for Molecular Developmental Biology, Department of Biophysics, Kyoto University, Kitashirakawa-Oiwake-tyo, Sakyo-ku, Kyoto 606-8502, Japan. [4]Temasek Life Sciences Laboratory and Department of Biological Sciences, 1 Research Link, National University of Singapore, Singapore 117604, Singapore.

*Author for correspondence (nfuse@gcoe.biol.sci.kyoto-u.ac.jp)

Accepted 1 August 2013

Heterotrimeric G proteins are GTP-binding signaling complexes that consist of Gα, Gβ and Gγ subunits (Neer, 1995). They are involved in diverse biological processes, such as phototransduction and chemotaxis. Numerous studies have revealed that G protein signaling can be regulated positively or negatively by many factors. Such adjustments of cell signaling guarantee its sensitivity and robustness (Ross, 2008). The roles of G protein regulators in development are poorly understood. Ric-8 is a putative guanine nucleotide-exchange factor for G protein (Tall et al., 2003), and *Drosophila* Ric-8 plays important roles during mesoderm invagination (Kanesaki et al., 2013). GPCR kinase (also known as GRK) is another example of a G protein regulator (Pitcher et al., 1998; Penn et al., 2000). GPCR kinase phosphorylates ligand-stimulated GPCR and attenuates its signaling (Moore et al., 2007). Consequently, GPCR kinase provides a negative-feedback loop for G protein signaling. For instance, mouse *Grk1* knockout retinal cells produce stronger and longer outputs upon receiving a flash of light (Chen et al., 1999), suggesting that GRK1 regulates the sensitivity and duration of signaling. Recently, it has been shown that a *Drosophila* GPCR kinase, Gprk2, plays diverse roles in various biological processes, such as egg morphogenesis, olfactory response and tissue patterning (Schneider and Spradling, 1997; Molnar et al., 2007; Tanoue et al., 2008; Chen et al., 2010; Cheng et al., 2012). However, the role of Gprk2 in embryonic development has remained unclear.

Here we show that *Drosophila* Gprk2 is essential for the process of gastrulation. In *Gprk2* mutant embryos, the apical constriction was abnormally expanded to the whole mesoderm and the involution movement was abolished. We propose that two types of cell movement – apical constriction in VM cells and involution in LM cells – are directed by the adjustment of G protein signaling.

MATERIALS AND METHODS

Fly strains

Drosophila melanogaster strains used in this study were *gprk2*^{6936} (Schneider and Spradling, 1997), *cta*^{RC10} (Parks and Wieschaus, 1991), *fog*^{4a6} (Costa et al., 1994), P{Moe::GFP} (Kiehart et al., 2000), P{Sph::GFP} (Royou et al., 2002) and P{Matα4-Gal4-VP16} (kindly provided by D. St Johnston, University of Cambridge, UK). *w*^{1118} was used as the wild-type control strain. Flies were reared with a standard cornmeal medium at 25°C.

To make the UAS-Gprk2 transgenic strain, part of the coding region of *Gprk2* was amplified by PCR from an EST clone (RE34982) and then subcloned into the pUASt vector. The UAS-Gprk2 K338R mutant was made by site-directed mutagenesis using a *Dpn*I mutagenesis kit (Stratagene). Sequences of coding regions were confirmed for both constructs, and plasmids were injected together with helper plasmid (Δ2-3) into *w*^{1118} embryos. Transgenic strains were established, and expression of transgenes was confirmed by *in situ* hybridization. We also made the UAS-Cta and the UAS-Cta Q303L transgenic strains in a similar way. An EST clone (LD04530) was used as starting material. Antibody staining confirmed the expression of the transgenes.

Antibodies

The antibodies used in this study were anti-Eve, anti-Dl, anti-Dlg, anti-Sxl, anti-DE-Cadherin (obtained from DSHB), anti-β-gal (mouse antibody from Promega; rat antibody kindly provided by T. Isshiki, National Institute of Genetics, Japan), anti-α-Tubulin (Sigma), anti-aPKC (Santa Cruz), anti-Zip (kindly provided by F. Matsuzaki, RIKEN, Japan), anti-Mir (Ikeshima-Kataoka et al., 1997), anti-Cta (Kanesaki et al., 2013) and anti-Twi (Roth et al., 1989).

To produce antibody against Fog, the full-length Fog ORF was amplified from an EST clone (SD02223) by PCR and subcloned into the pQE80 vector (Qiagen). The recombinant protein was expressed in *E. coli* and purified from lysate using Ni-NTA resin (Qiagen). The purified protein was injected into a rabbit and antiserum was prepared by MBL. The antiserum was affinity purified using the antigen. The antibody staining of embryos reproduced the pattern of *fog* RNA expression (see also Ratnaparkhi and Zinn, 2007).

Genetic experiments

Embryos maternally and zygotically mutant for *Gprk2* were collected from mating between *gprk2*^{6936} homozygous females and males. For rescue experiments of the *Gprk2* mutant, we set up a cross between P{Matα4-Gal4-VP16}/CyO; *Gprk2*/*Gprk2* females and P{UAS-Gprk2 (wild-type or K338R)}; *Gprk2*/*Gprk2* males, and collected embryos.

To make a double mutant for *fog* and *Gprk2*, embryos were collected from mating between *fog*/FM7 P{ftzlacZ}; *Gprk2*/*Gprk2* females and +/Y; *Gprk2*/*Gprk2* males, and were stained with β-gal antibody (to distinguish between the embryos with the *fog* and FM7 chromosome) and Sxl antibody (to distinguish between the embryos with + and the Y chromosome). The embryos negative for β-gal and Sxl were judged to be *fog Gprk2* double mutants, and the embryos negative for β-gal and positive for Sxl were judged to be *Gprk2* mutants carrying one copy of the *fog* gene. We also collected embryos from mating between *fog*/FM7 P{ftzlacZ} females and +/Y males for a control experiment.

To examine the effects of overexpression of Cta and Gprk2, we set up a cross between P{Matα4-Gal4-VP16} females and P{UAS-Cta} males or P{UAS-Gprk2}; P{UAS-Cta} males, and collected embryos. Since P{UAS-Cta Q303L} was homozygous lethal, we used P{UAS-Cta Q303L}/CyO males for experiments. Embryos carrying P{UAS-Cta Q303L} were judged by severe malformation, which was never observed in embryos collected from P{Matα4-Gal4-VP16} females and the wild-type males.

Analyses of fixed embryos

For scanning electron microscopy (SEM), embryos were fixed as previously described (Kanesaki et al., 2013). Ion-coated embryos were observed using a JEOL JSM-7500F scanning electron microscope.

For immunostaining analysis, embryos were fixed and stained as described (Kanesaki et al., 2013). To acquire images, we mainly used confocal laser scanning microscopy (Carl Zeiss LSM5 Live or Olympus FV10). Alternatively, we used spinning disk microscopy (Olympus DSU system) for the images of Fig. 7 and supplementary material Figs S3 and S5. Stacked images along the *z*-axis were merged by maximum intensity projection using the LSM Image Browser (Carl Zeiss) or MetaMorph (Molecular Devices). Images were processed using ImageJ (NIH) and Photoshop (Adobe).

For *in situ* hybridization analysis, embryos were fixed twice and hybridized with Dig-labeled RNA probes (Roche) according to the standard protocol. Alkaline phosphatase was used to detect Dig probes, and embryos were stained with NBT/BCIP solution (Roche). Stained embryos were observed using a differential interference contrast (DIC) microscope (Olympus BX63).

Analyses of live embryos

Analysis of live embryos was performed as described (Kato et al., 2004). Briefly, dechorionated embryos were attached to a cover glass coated with rubber glue. A plastic slide with a 5-mm diameter hole was placed on the cover glass, and the hole was filled with silicon oil (Shin-Etsu Chemical). After incubation of embryos in a humidified chamber for an appropriate time, embryos were observed under a Zeiss LSM5 Live microscope at room temperature (controlled at 24±3°C). Images were processed using LSM Image Browser, ImageJ and Photoshop.

To quantify cell movements in the wild-type embryos, time zero was taken as the time when gastrulation started (some change in cell shape was visible). To compare *Gprk2* mutant with wild-type embryos, we observed the cellularization process and determined time zero as the time when furrow canals of cells reached 12 μm in depth. This time zero corresponds to ~5 minutes before gastrulation starts.

Quantitative analysis of cell movement was performed using the manual tracking plug-in of ImageJ. A clearly visible lateral vertex of a cell was chosen, and the trajectory of the cell vertex was tracked. The cell vertex frequently became unclear at the late stage of invagination. In such cases, we deduced the cell vertex by judging from the sequential timecourse images. The final destination of each cell before it disappeared from an image was defined as the end position, and distances of the trajectory to the

end position were quantified. Data were processed using Excel (Microsoft) and R (http://www.r-project.org/).

A kymograph was constructed from time interval stacked images. A slit along the dorsoventral axis was chosen and the slits of images were aligned along the timecourse using the Reslice function of ImageJ.

RESULTS

Lateral mesodermal cells extend apical protrusions and display two phases of movement

To characterize the cell movements during mesoderm invagination, we first observed the cell morphology of embryos by SEM (Fig. 1A). As previously described (Costa et al., 1993), VM cells flatten and constrict their apical cell surface to make the ventral furrow (Fig. 1A, yellow), but LM cells do not undergo such apical constriction. We then observed that LM cells extended thin protrusions (several microns long) toward the mid-ventral region (Fig. 1A, red). The stretching of LM cells toward the mid-ventral region has been reported previously (Turner and Mahowald, 1977; Costa et al., 1993; Fox and Peifer, 2007), but the morphology and behavior of the protrusions have not been characterized in detail. The protrusions were not restricted to LM cells, as cells in more lateral regions, most likely ectodermal cells, also extended protrusions (Fig. 1A, blue), although these protrusions were much shorter than those of LM cells.

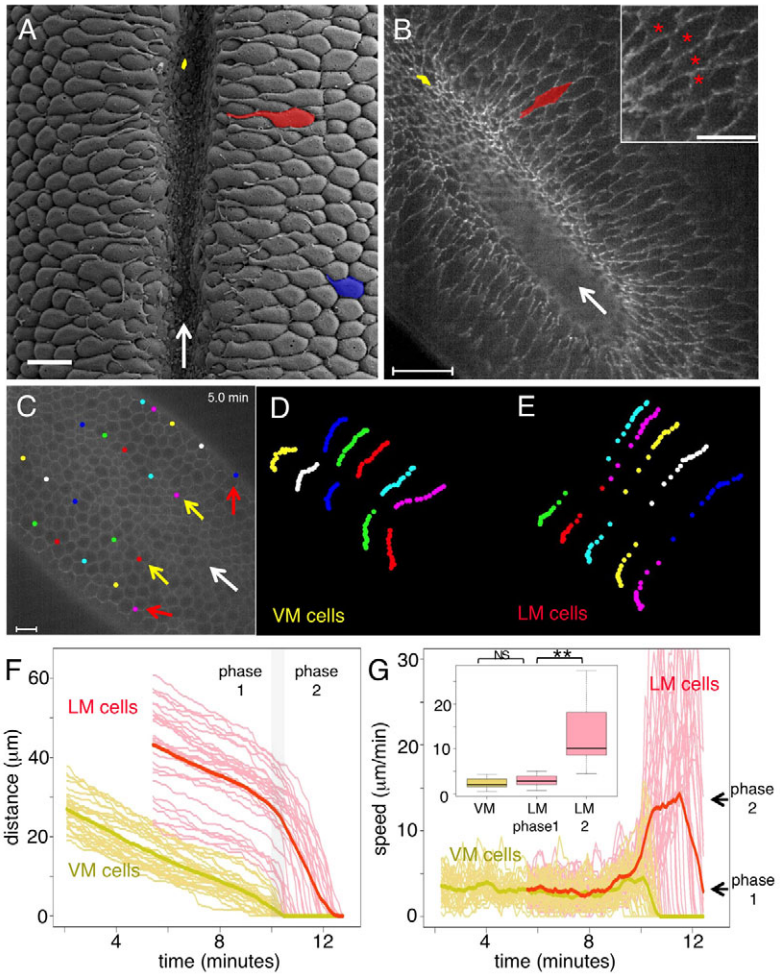

Fig. 1. Cell morphology and movements during *Drosophila* gastrulation. (**A**) SEM image of a wild-type embryo at gastrulation stage. Ventral view, with anterior to the top (all subsequent images are of the same orientation unless stated otherwise). The ventral furrow forms along the anteroposterior axis (arrow). Ventral mesodermal (VM), lateral mesodermal (LM) and ectodermal cells are pseudocolored yellow, red and blue, respectively. (**B**) A ventral view of the posterior region of a live Moe::GFP embryo (supplementary material Movie 1). Focus was adjusted to the surface of the embryo. Arrow indicates the ventral furrow and points to anterior. Inset is a high-magnification view of LM cells (see supplementary material Movie 2). LM cells bearing protrusions are marked with asterisks. (**C**) An example of tracking of cell movements in a Moe::GFP embryo (supplementary material Movie 3). Images were focused at 7 μm depth. Anterior is to the upper left (white arrow). The cell vertexes chosen for tracking are marked with colored dots. Yellow and red arrows represent VM and LM cells, respectively. (**D**,**E**) Tracking of movements of VM (D) and LM (E) cells. The positions of cells at 30-second intervals are superimposed. Whereas the speed of VM cells was generally constant, LM cells accelerated when they neared the mid-ventral region. (**F**) Quantification of the movements of VM (yellow) and LM (red) cells. The timecourse of the distance from the final destination for each cell was plotted. The movements of 30 cells in three embryos are shown in light colors, and the average movements are shown in dark colors. The movement of LM cells can be divided into two phases. (**G**) The speed at 5-second steps over a period of 30 seconds is plotted against time for each cell (light colors), with the mean speed for all 30 cells (dark colors). The two phases of LM movement are indicated by arrows on the right. Inset shows the speeds during a 1-minute period (7-8 minutes for VM and LM phase 1, and 10.5-11.5 minutes for LM phase 2) as a box plot. The difference between LM phase 1 [2.9±1.2 μm/minute (mean ± s.d.)] and phase 2 (12.7±6.1 μm/minute) was statistically significant (**P<0.01, n=30 cells, Welch's t-test), but that between the VM (2.5±1.1 μm/minute) and LM phase 1 was not significant (NS). Scale bars: 10 μm in A,C,B inset; 20 μm in B.

We next performed live imaging of the cell movements in embryos expressing Moe::GFP, a fluorescent marker that binds to actin filaments (Kiehart et al., 2000) (supplementary material Movie 1). From the sequence of images, we defined VM cells (apical constricting ventral cells) and LM cells (involuting lateral cells), and analyzed their morphologies and movements. As the apical constriction proceeded in VM cells, we observed thin protrusions extending from the LM cells, as also seen by SEM (Fig. 1B). The protrusions shook and moved dynamically back and forth (supplementary material Movies 1, 2; compare left and right images focused on the apical surface and at 9 μm depth of the same embryo). Since the protrusions were observed only at the plane of the most apical surface, we termed this structure the 'apical protrusion'. We also found that the apical protrusions could be visualized by immunostaining for α-Tubulin (supplementary material Fig. S1), suggesting that cytoskeletal filaments (microfilaments and microtubules) actively support the protrusions on the apical cell membrane.

We also quantified the cell movements using Moe::GFP embryos (Fig. 1C-E; supplementary material Movie 3). While the apical constriction proceeded, LM cells moved toward the mid-ventral position with a mean speed of 2.9 μm/minute (Fig. 1F,G, phase 1), which roughly corresponds to the speed of VM cells (2.5 μm/minute). After the apical constriction was completed, the movement of LM cells accelerated to 12.7 μm/minute (Fig. 1F,G, phase 2). These observations demonstrate that there are two phases of LM movements (Fig. 1G, inset). The apical protrusions became apparent just before LM cells started the accelerated movement, suggesting the possibility that the protrusions contribute to the involution movement of LM cells (see Discussion). Thus, during mesoderm invagination, two cell groups (VM and LM cells) display different morphologies of the apical cell surface (flat surface and apical protrusion, respectively) and undergo distinct cell movements (apical constriction and involution, respectively). It was hitherto unknown how these distinct cell movements are spatially organized in presumptive mesodermal cells.

Gprk2 is required for gastrulation

To elucidate the molecular mechanism underlying these cell movements, we searched for new factors involved in the G protein signaling pathway during gastrulation, and found that a *Drosophila* GPCR kinase, Gprk2, acts in the process. *gprk2*^{6936} is a female-sterile mutant carrying a P-element insertion that abolishes the maternal expression of *Gprk2* in developing eggs (Schneider and Spradling, 1997) (supplementary material Fig. S2E). We collected embryos maternally and zygotically mutant for *gprk2*^{6936} (referred to simply as *Gprk2* mutant hereafter) and observed them by SEM (Fig. 2). Although the *Gprk2* mutant embryos displayed a rounded overall shape, as reported previously (Schneider and Spradling, 1997), cellularization proceeded normally in the mutant. We then observed abnormal gastrulation in *Gprk2* mutant embryos (Fig. 2E-G): the apical constricting area represented by a flattened surface was abnormally expanded (Fig. 2H, yellow bars). Although the cells lateral to the furrow extended apical protrusions (Fig. 2H, arrow), these cells were thought to be ectodermal cells, as described below. At a later stage (germ band extension), about two-thirds of the mutant embryos (11 of 15) exposed the mesoderm to the outside (Fig. 2G), although other embryos did finally close the furrow. The *Gprk2* mutant also displayed abnormal positioning of germ cells (Fig. 2F, arrow). This phenotype might be due to the expansion of the posterior midgut invagination together with the ventral furrow.

Staining for Dorsal (ventral region), Even-skipped (segmental stripes) and Twi (mesoderm) proteins showed that the *Gprk2* mutant establishes axial patterning and allocates mesodermal cells normally (supplementary material Fig. S2). Staining for DE-Cadherin (Shotgun – FlyBase) and aPKC proteins showed that the *Gprk2* mutant has normal adherens junctions and apicobasal cell polarity (supplementary material Fig. S2). These results indicate that the gastrulation phenotypes in the *Gprk2* mutant are due to impaired cell movements.

We established transgenic fly lines carrying UAS-Gprk2 and observed that the exogenous Gprk2 expression rescued the expansion of the ventral furrow in the *Gprk2* mutant embryos, confirming that Gprk2 is required for mesoderm invagination (supplementary material Fig. S3). In this condition, the apical constriction was occasionally blocked in some regions (supplementary material Fig. S3C, arrow), suggesting that excess Gprk2 activity might inhibit the apical constriction.

To examine the role of the kinase activity of Gprk2 *in vivo*, we made a Gprk2 construct carrying a point mutation (K338R), which

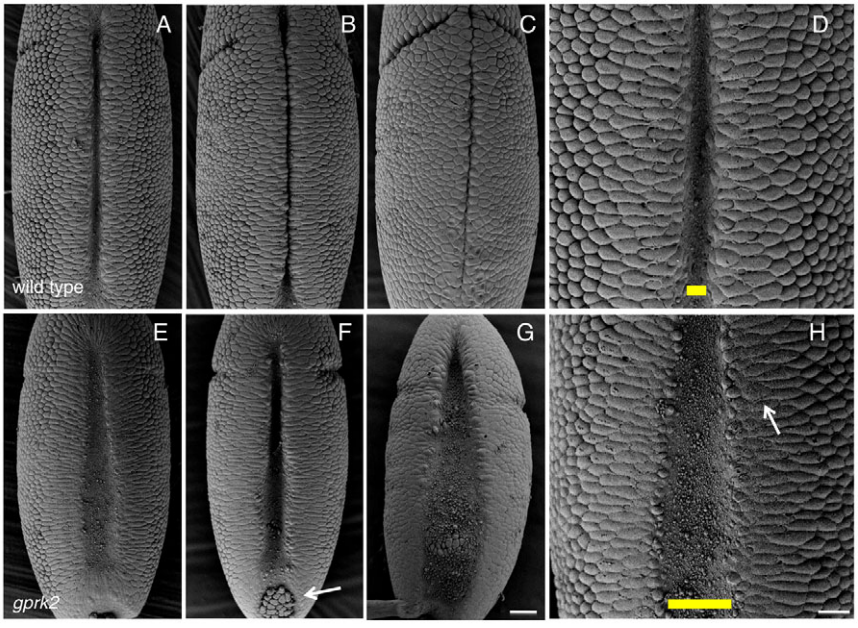

Fig. 2. SEM analysis of *Gprk2* mutant embryos. (**A-C**) SEM images of wild-type *Drosophila* embryos at middle (A) and late (B) stage of gastrulation, and at early germ band elongation stage (C). (**D**) A high-magnification view of a wild-type embryo at middle stage. (**E-H**) SEM images of *Gprk2* mutant embryos (in the same order as A-D). Apical constricting areas are shown by yellow bars. Arrows in F and H indicate abnormal positioning of germ cells and a short protrusion extended from an ectodermal cell, respectively. Scale bars: 20 μm in G; 10 μm in H.

is analogous to the kinase dead mutations of other GPCR kinases (Lee et al., 2004). In contrast to the wild-type Gprk2 protein, the K338R mutant protein did not rescue the *Gprk2* mutant phenotypes (supplementary material Fig. S3D). Thus, the kinase activity of Gprk2 is essential for its function during gastrulation.

Apical constriction is expanded to the whole mesoderm in the *Gprk2* mutant

In *Gprk2* mutant embryos, the ventral furrow was abnormally expanded (Fig. 2H). There could be two possible explanations for this: more cells might undergo apical constriction and/or the apical constriction might be incomplete. To examine the first possibility, embryos were stained for Twi and Zipper (Myosin heavy chain) and transverse sections of the embryos examined (Fig. 3). In the wild-type embryos, ~12 cells in the middle of the Twi-positive (VM) cells constrict their surfaces to form the ventral furrow, and two to three cells on the sides of the Twi-positive region (LM cells) do not descend into the furrow (Fig. 3A,C). In VM cells, Myosin was translocated from the basal (inside) to the apical (outside) surface (Fig. 3G, arrowhead). In *Gprk2* mutant embryos, however, the ventral furrow was expanded to include all of the Twi-positive cells (Fig. 3D) and the apical Myosin was also expanded to all cells in the furrow (generally 16 to 18 cells; Fig. 3H, arrowhead), indicating that the apical constriction is expanded to the whole mesoderm in the mutant (Fig. 3B). This notion was also supported by two additional features of apically constricting cells: expansion of the basal cell surface and the basal displacement of nuclei (Costa et al., 1993; Gelbart et al., 2012). At later stages, the ventral furrow frequently remained open as a U-shaped furrow in the mutant (Fig. 3F). Thus, all of the mesodermal cells undergo apical constriction in the *Gprk2* mutant, suggesting that Gprk2 normally inhibits the apical constriction in LM cells, such that apical constriction is restricted to VM cells.

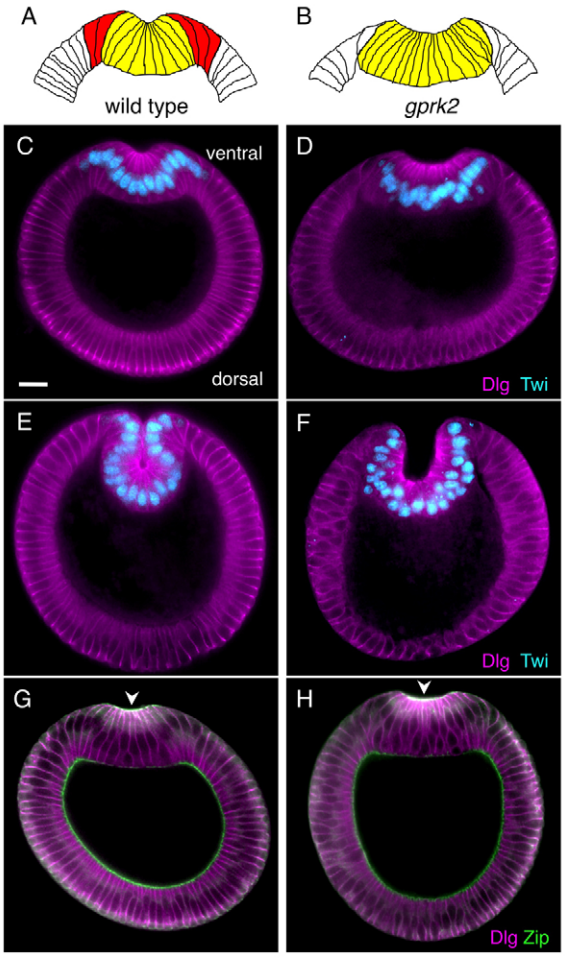

Fig. 3. Analyses of transverse sections of embryos. (**A**,**B**) Schematic representations of transverse sections of wild-type (A) and *Gprk2* mutant (B) *Drosophila* embryos. Apical constricting and non-constricting mesodermal cells are yellow and red, respectively. (**C-H**) Transverse sections of wild-type (C,E,G) and *Gprk2* mutant (D,F,H) embryos stained for Dlg and Twi (C-F) and for Dlg and Zip (G,H) proteins. Embryos were at early (G,H), middle (C,D) and late (E,F) stages of gastrulation. Arrowheads indicate apically localizing Zip. Ventral side is to the top for all images. Scale bar: 20 μm.

Apical constriction fails to complete in the *Gprk2* mutant

To examine whether the apical constriction is incomplete in the *Gprk2* mutant, we performed live imaging of the embryos using Moe::GFP (Fig. 4; compare supplementary material Movie 5 with Movie 4 of the control embryo). We confirmed that all mesodermal cells (an ~18-cell width) start to constrict their apical cell surfaces mostly simultaneously in the mutant (Fig. 4C′). Ectodermal cells on the sides of the mesoderm extended apical protrusions but never underwent involution movement. We made kymographs from time interval images to characterize the trajectory of cell movements, and this analysis also showed two phases of movement of the wild-type LM cells (Fig. 4B, red arrows; compare with Fig. 1F). In the *Gprk2* mutant, the width of the mesodermal cell region was approximately halved within 3 minutes (roughly estimated speed of cell movement: 6 μm/minute), which was almost twice as fast as that of the wild type (see Fig. 4B,D, yellow arrows; slopes of cell trajectory represent the speed of cell movements). Thereafter, the apical constriction ceased prematurely and never resumed in the mutant (Fig. 4C″,D, yellow arrowhead), suggesting that Gprk2 is required for completion of apical constriction.

We examined the dynamics of Myosin, which is a primary force generator for apical constriction, using Sqh::GFP [Myosin light chain fused to GFP (Royou et al., 2002)]. In this experiment, we started the observations from the cellularization process and took time zero as that when cellularization was completed (~5 minutes before gastrulation; see Materials and methods) in order to examine the timing of changes in Myosin localization. It has been reported that Myosin is initially localized as particles and later forms a supracellular meshwork to generate tension acting throughout the tissue (Martin et al., 2009; Martin et al., 2010) (Fig. 5A; supplementary material Movie 6). In the *Gprk2* mutant, the Myosin accumulation started earlier than in the control (at 2 minutes in the *Gprk2* mutant versus 5 minutes in the control; Fig. 5B; supplementary material Movie 7), and Myosin continued to accumulate on the apical surface of the mutant cells (Fig. 5B′, inset). This aberrant accumulation of Myosin might cause the premature termination of apical constriction in the mutant. Thus, Gprk2 is required for the localization and kinetics of Myosin accumulation in apically constricting cells.

Gprk2 mutant phenotypes are dependent on the *fog* gene

The expansion of the apical constricting area and the abnormal accumulation of Myosin in the *Gprk2* mutant are similar to the phenotypes of Fog overexpression (Morize et al., 1998; Dawes-Hoang et al., 2005). However, there is a significant difference

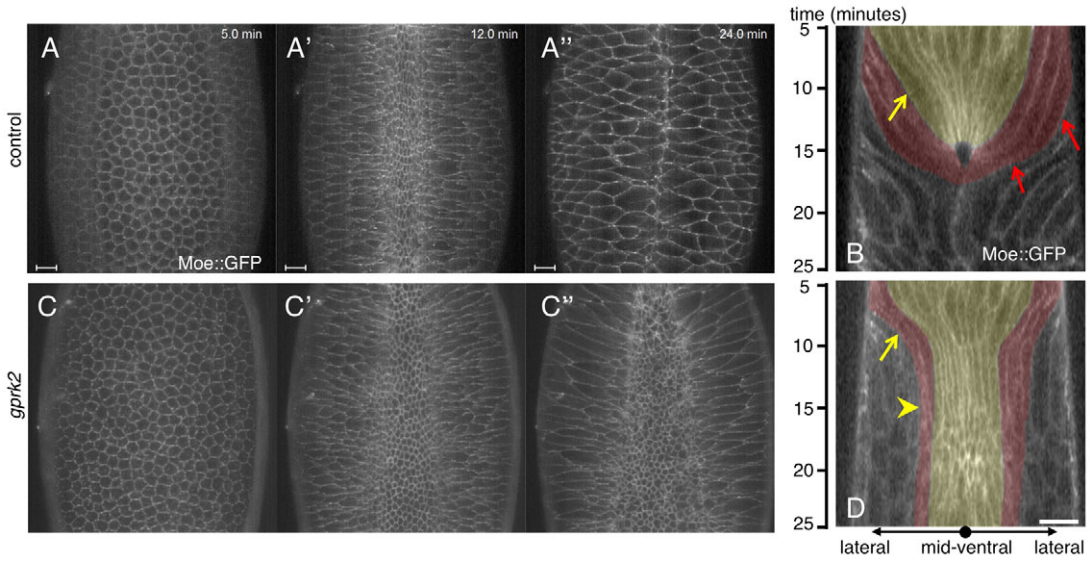

Fig. 4. Live imaging analysis of cell movements in *Gprk2* mutant embryos. (**A-A″**) Montage of movie (supplementary material Movie 4) showing a live Moe::GFP *Drosophila* embryo in ventral view. Five stacked images along the *z*-axis (4 µm depth) were merged. (**B**) Kymograph constructed from time interval stacked images. The mid-ventral region is located at the center of the image. Cells located in the VM and LM areas are pseudocolored yellow and red, respectively. The trajectory of cell movements during apical constriction is indicated by the yellow arrow. Red arrows indicate the two phases of movement of LM cells. (**C-C″**) Montage of movie (supplementary material Movie 5) showing a live *Gprk2* mutant embryo with Moe::GFP in ventral view. (**D**) Kymograph constructed similarly to that in B. Apical constriction ceased prematurely (arrowhead). Scale bars: 10 µm in A-A″; 20 µm in D.

between the two: apical Myosin accumulates only in mesodermal cells in the *Gprk2* mutant (Fig. 3H) but in all cells in the embryo with Fog overexpression (Dawes-Hoang et al., 2005). These observations suggest that Fog signaling might be activated in mesodermal cells of the *Gprk2* mutant.

To examine the relationship between Fog and Gprk2, we made a double mutant for *fog* and *Gprk2* (Fig. 6; see Materials and methods). Embryos were stained with β-gal and Sxl antibodies

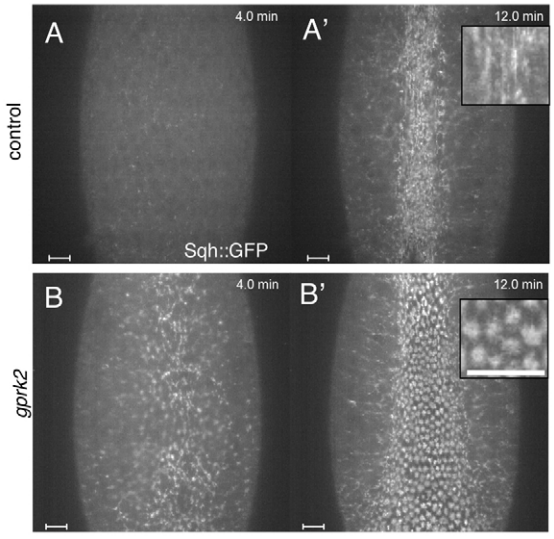

Fig. 5. Live imaging analyses of Myosin localization. (**A**,**A′**) Montage of movie (supplementary material Movie 6) of a live control (*Gprk2* heterozygous) *Drosophila* embryo carrying Sqh::GFP. (**B**,**B′**) Montage of movie (supplementary material Movie 7) of a live *Gprk2* (homozygous) mutant embryo carrying Sqh::GFP. Insets are high-magnification views of the furrow regions of A′ and B′. Scale bars: 10 µm.

(chromosome markers) to judge the genotype of the embryos. The *fog Gprk2* double-mutant embryos showed only a few apically constricting cells at random positions (Fig. 6F), which is essentially the same phenotype as that of the *fog* single mutant (Fig. 6C). This indicates that the *Gprk2* phenotypes are dependent on the *fog* gene, and is consistent with our idea that Gprk2 acts on Fog signaling. In addition, we examined *Gprk2* mutant embryos carrying one copy of the *fog* gene. In these embryos (+/*fog*; *Gprk2*/*Gprk2* genotype), apical constriction was substantially disorganized and asynchronous among mesodermal cells, compared with that in the *Gprk2* single mutant (Fig. 6E compared with 6D). By contrast, the *fog* heterozygous embryos with the *Gprk2*-plus background (+/*fog* genotype) showed mostly normal invagination, as in the wild-type embryos (Fig. 6B compared with 6A). These results indicate that the *Gprk2* mutant is sensitive to the dose of the *fog* gene and suggest that Gprk2 adjusts Fog signaling to an appropriate level from either one or two copies of the *fog* gene.

We next examined the expression of Fog in the *Gprk2* mutant. In wild-type embryos, *fog* RNA is expressed at the ventral region, mostly in VM cells (Costa et al., 1994). However, we observed that not all VM cells express *fog* RNA; rather, *fog*-positive and *fog*-negative cells were intermingled in the VM area, and the same was true in the LM area (supplementary material Fig. S4A; the *fog*-expressing area was ~18 cells wide). This expression pattern of *fog* RNA was not altered in the *Gprk2* mutant (supplementary material Fig. S4C). We then raised an antibody to examine the localization of Fog protein. At the subcellular level, Fog was detected mostly in puncta in the cytoplasm (supplementary material Fig. S4B), as previously reported (Dawes-Hoang et al., 2005). At the tissue level, Fog protein was detected in a mosaic pattern in mesodermal cells, consistent with its RNA expression. In the *Gprk2* mutant, Fog was expressed in a similar pattern to that in the wild-type embryo (supplementary material Fig. S4D), although, at the late stage of

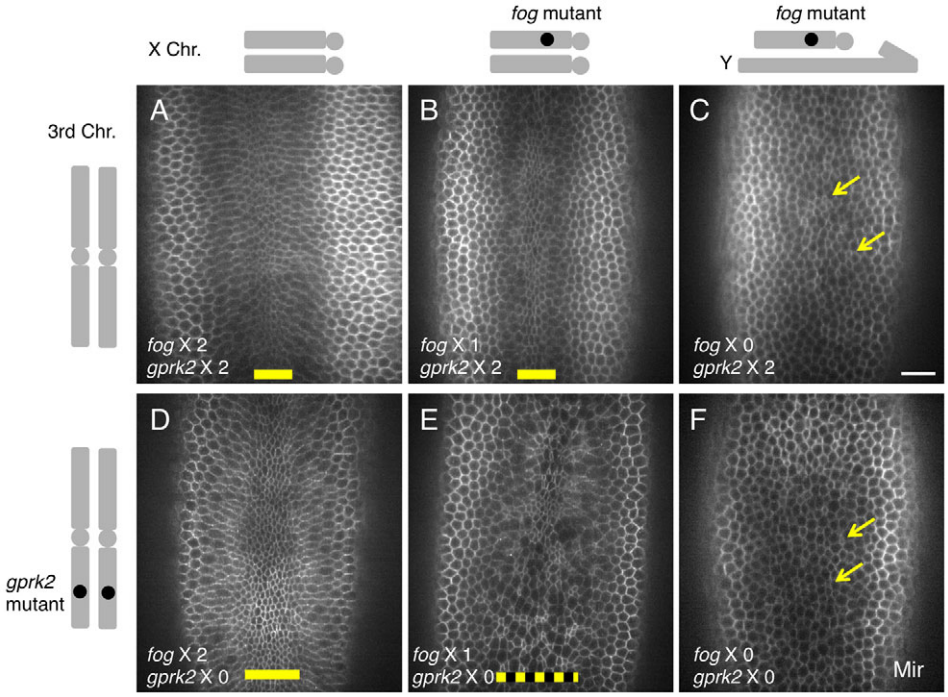

Fig. 6. Phenotype of *Gprk2 fog* double-mutant embryos. *Drosophila* embryos were stained for Miranda (Mir) protein. Genotypes of the embryos are (**A**) wild type, (**B**) *fog/+*, (**C**) *fog/Y*, (**D**) *Gprk2/Gprk2*, (**E**) *fog/+; Gprk2/Gprk2*, (**F**) *fog/Y; Gprk2/Gprk2* and are represented by the schematics alongside. The gene doses of *fog* and *Gprk2* are indicated in the bottom left corner of each image. Apically constricting areas are indicated by yellow bars and uncoordinated apical constrictions are indicated by arrows. Scale bar: 20 μm.

gastrulation, somewhat more Fog staining was seen than in the wild type. From these data, we suggest that Gprk2 primarily regulates Fog signaling rather than the expression of Fog protein.

Overexpression of Gprk2 suppresses the effects of excess Cta

To obtain further evidence for the function of Gprk2 in Fog signaling, we examined the functional interactions between Gprk2 and Cta, a downstream component of Fog signaling. We made transgenic fly lines carrying UAS-Cta and observed the effects of Cta expression driven by Matα4-Gal4-VP16 (hereafter termed as Maternal-Gal4). Overexpression of Cta compromised the gastrulation process, causing, for example, partial disruption of the ventral furrow (Fig. 7C), although the phenotypes were varied among the embryos (e.g. delay of furrow closure and ectopic folding of the lateral ectodermal cells). In such embryos, Myosin had accumulated abnormally on the apical surface of the lateral ectodermal cells (Fig. 7D), similar to in *Gprk2* mutant mesodermal cells (Fig. 5B). This suggests that Cta overexpression induces ectopic signaling in ectodermal cells, as previously reported (Morize et al., 1998; Rogers et al., 2004). We then examined simultaneous overexpression of Cta and Gprk2. The effects of Cta overexpression were largely suppressed by simultaneous expression of Gprk2 (Fig. 7G,H). Overexpression of Gprk2 alone did not severely affect furrow closure or overall Myosin localization (Fig. 7E,F), although it partially inhibited apical constriction, as seen in the rescue experiment (supplementary material Fig. S3). Furthermore, the lethality of Maternal-Gal4/UAS-Cta individuals was suppressed by simultaneous expression of Gprk2 [from 73% (n=131) to 27% (n=135), as judged by the ratios of adults with or without the transgene]. These results suggest that Gprk2 attenuates Cta signaling.

We next performed a similar experiment using a point mutant of Cta (Q303L), which is analogous to the constitutively active mutant

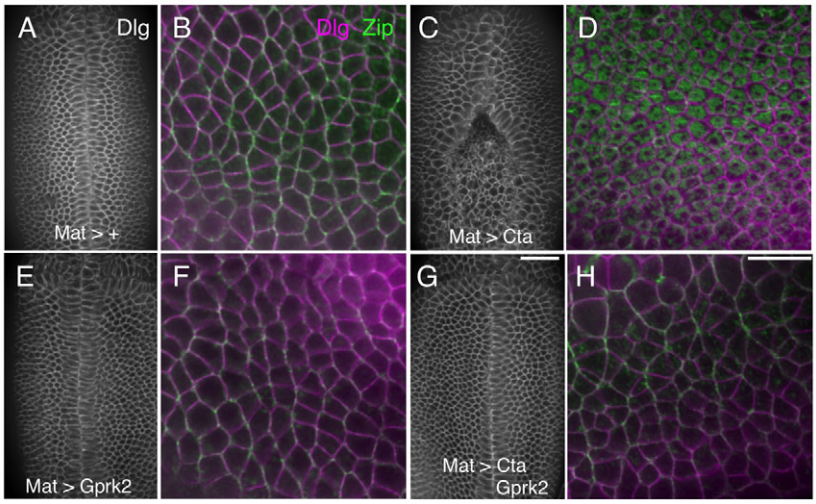

Fig. 7. Simultaneous overexpression of Cta and Gprk2. (**A**,**C**,**E**,**G**) *Drosophila* embryos at late gastrulation stage stained for Dlg protein. (**B**,**D**,**F**,**H**) High-magnification views of the apical surface of lateral ectodermal cells stained for Dlg and Zip proteins. Anterior is to the left and dorsal is to the top. Genotypes are Maternal-Gal4 (A,B), Maternal-Gal4, UAS-Cta (C,D), Maternal-Gal4, UAS-Gprk2 (E,F) and Maternal-Gal4, UAS-Cta, UAS-Gprk2 (G,H). Scale bars: 20 μm in G; 10 μm in H.

in which Cta is fixed to the GTP-bound form of Gα protein (Grishina and Berlot, 1998). Overexpression of Cta Q303L resulted in severe malformation of the embryo (supplementary material Fig. S5A). Myosin accumulated strongly in the lateral cell cortex, and the epithelial architecture seemed to have collapsed (supplementary material Fig. S5B). These phenotypes could be explained by the perturbation of signaling due to constitutive Cta activity. Overexpression of Gprk2 did not suppress the effects of Cta Q303L (supplementary material Fig. S5C,D), suggesting that Gprk2 regulates Fog-Cta signaling before the activation of Cta effectors. Together, these data suggest that repression of Cta activity might be one mode by which Gprk2 regulates Fog signaling.

DISCUSSION

We characterized the cell movements in *Drosophila* mesoderm invagination and examined the roles of a GPCR kinase, Gprk2, in this process. We found that two cell groups (VM and LM cells) among mesodermal cells undergo distinct cell movements, and Gprk2-adjusted Fog signaling defines the areas of these two cell groups. Thus, these two different cell movements in mesoderm invagination are not predetermined, but rather are organized by the adjustment of Fog signaling.

Molecular functions of Gprk2 in gastrulation

In the *Gprk2* mutant embryos, cell movements triggered by Fog signaling were compromised. We found that *fog* is genetically epistatic to *Gprk2*, indicating that Gprk2 functions by acting on Fog signaling. LM cells undergo apical constriction in the *Gprk2* mutant, suggesting that Gprk2 normally inhibits Fog signaling in LM cells. We also observed premature termination of apical constriction and abnormal accumulation of Myosin in the *Gprk2* mutant, suggesting that Gprk2 adjusts Fog signaling to an appropriate level in VM cells. Thus, Gprk2 regulates Fog signaling in a cell group-dependent manner. But what are the underlying molecular mechanisms?

It is known that GPCR kinase phosphorylates the C-terminal region of GPCR, and regulates GPCR signaling by multiple mechanisms (Penn et al., 2000; Moore et al., 2007). The phosphorylated GPCR dissociates from the G protein and is internalized from the plasma membrane. This produces a negative-feedback loop for GPCR signaling. Theoretically, the negative-feedback loop stabilizes the signaling and generates biphasic output from fluctuating inputs: OFF for low inputs and ON for high inputs (Brandman and Meyer, 2008). We speculate that Gprk2 might phosphorylate a GPCR and might generate biphasic output for Fog signaling in a spatial manner: OFF in LM cells and ON in VM cells. The Fog receptor is expected to be a GPCR, since a G protein (Cta) functions downstream of Fog (Parks and Wieschaus, 1991). Identification of the Fog receptor would help to clarify the molecular functions of Gprk2.

The kinase activity of Gprk2 is essential for gastrulation. Although we do not yet know what substrates are phosphorylated by Gprk2 in this process, one might be Gprk2 itself because we observed that Gprk2 protein was phosphorylated in S2 cultured cells and that the phosphorylation was abolished in the K338R mutant of Gprk2 (N.F., unpublished data). Autophosphorylation of other GPCR kinases has been demonstrated previously and is thought to stimulate their binding to GPCR (Pitcher et al., 1998). Autophosphorylation of Gprk2 might play a similar role.

In addition to its kinase activity, GPCR kinase has an RGS domain, which exhibits GAP (GTPase activating protein) activity and functions in recycling of the Gα protein (Pitcher et al., 1998; Penn et al., 2000). Therefore, whether Gprk2 exhibits GAP activity for Cta is an intriguing issue. Indeed, this possibility was supported by our genetic data showing that Gprk2 suppresses the effect of Cta overexpression, but not that of Cta Q303L, the GTP-bound form of Cta protein. Cta Q303L might not be subject to the inhibitory effect (GAP activity) of Gprk2, although we have not ruled out the alternative explanation that the inhibition of Cta Q303L might require more Gprk2 protein than does the inhibition of wild-type Cta. Considering that GPCR kinase regulates GPCR signaling by multiple mechanisms, we suggest that the repression of Cta activity might be one of several means by which Gprk2 regulates Fog signaling.

Fog signaling stimulates the apical localization of Myosin, which generates a force to constrict the apical cell surface. Martin et al. (Martin et al., 2009) observed that, in the wild-type embryo, Myosin protein appears and disappears at the apical surface in a dynamic pattern that they described as ‘pulsed coalescence’. In the *Gprk2* mutant, Myosin continued to accumulate on the entire apical surface of mesodermal cells. We also observed similar phenomena in Cta-overexpressing ectodermal cells, and this phenotype was suppressed by simultaneous expression of Gprk2. We suggest that Gprk2 normally attenuates Fog-Cta signaling to an appropriate level, and such refinement might contribute to controlling the dynamics of Myosin protein.

Previous studies showed that Gprk2 acts in Hedgehog (Hh) signaling for imaginal disc patterning (Molnar et al., 2007; Chen et al., 2010; Cheng et al., 2012). In this process, Gprk2 phosphorylates a GPCR, Smoothened, and potentiates Hh signaling. Thus, Gprk2 plays roles in multiple signaling pathways in various contexts during development.

Sequential cell movements in mesoderm invagination

We characterized the movements of LM cells and found that they extended apical protrusions. Some examples have been documented of the extension of protrusions by epithelial cells, such as dorsal ectodermal cells of embryos and wing disc cells of larvae in *Drosophila* (Jacinto et al., 2000; Bosch et al., 2005). However, the mechanisms that induce the protrusion and the roles of protrusion in directional cell movement are not understood. Since we observed that apical protrusions in LM cells always pointed toward the ventral furrow and that cells close to the furrow extended longer protrusions than cells distant from it, we speculate that the apical protrusion might be induced by the apically constricting neighbors. Indeed, in *cta* mutant embryos the apical protrusions did not always point toward mid-ventral, but rather frequently pointed toward the slight depressions that were formed at random positions by uncoordinated apical constriction [data not shown; see also figure 4E in Kanesaki et al. (Kanesaki et al., 2013)]. One possibility is that mechanical or chemical signals that emanate from apically constricting cells might induce apical protrusions in surrounding cells.

Apical protrusions became apparent when LM cells started to accelerate toward the ventral furrow. From this observation, we suppose that the directional protrusion might contribute to the movement of LM cells. Given that the apical protrusion of LM cells is analogous to the pseudopod of cultured cells (Sánchez-Madrid and del Pozo, 1999), the apical protrusion might act as a scaffold for pulling the cell body into the furrow. The fact that the apical protrusion was also observed in some ectodermal cells, which never undergo involution movement, suggests that the apical protrusion is not sufficient to induce involution movement and that other mechanisms might regulate the cell movement in parallel.

Drosophila mesoderm invagination is driven by sequential movements of different cells (Costa et al., 1993). The apical constriction of VM cells is one of the essential movements in this process. We expect that the involution movement of LM cells might be another of the cell movements driving mesoderm invagination. The movements of different cells would probably influence each other in a complex manner. Our observations of LM movements might be explained by such a coordination of cell movements. For example, the apical constriction of VM cells might stretch LM cells and thereby prevent LM cell apical constriction, as previously suggested (Leptin and Roth, 1994). VM cells might then continue to move inward and pull LM cells toward the ventral furrow. In addition, ectodermal cells might generate a force to push mesodermal cells inward. These possibilities are not mutually exclusive. Further analyses are required to clarify the role of each cell movement and the effect of coordinated movements in mesoderm invagination.

In the *Gprk2* mutant, LM cells underwent apical constriction instead of involution movement. Given the inhibition of Fog signaling in the wild-type LM cells, involution movement might be a default state of mesodermal cells without Fog signaling. As noted above, in the *fog* and *cta* mutant, apical constriction occurs in some VM cells, and involution-like movement operates in an uncoordinated manner [data not shown; see also figure 4E in Kanesaki et al. (Kanesaki et al., 2013)]. These uncoordinated cell movements finally result in disorganized, but nearly complete, mesoderm invagination (Sweeton et al., 1991). Thus, apical constriction and involution movements seem to be alternative choices for mesodermal cells, as previously suggested (Leptin and Roth, 1994), and robust mesoderm invagination might progress via either type of cell movement. In normal *Drosophila* embryos, cell movements are spatially and temporally organized, and such organization might ensure the correct shape of gastrulae.

Cell movements in gastrulation show diversity among insects (Roth, 2004). For example, mosquito embryos undergo only apical constriction and no apparent involution process (Goltsev et al., 2007). Locust embryos undergo neither apical constriction nor involution, but instead utilize the delamination of individual mesodermal cells. Compared with gastrulation in these insects, *Drosophila* gastrulation is a more complex process and is completed within a shorter time (15 minutes compared with hours). The highly organized cell movements in *Drosophila* might enable this rapid completion of gastrulation. The molecular mechanisms underlying the evolution of insect gastrulation are an intriguing issue for future studies.

Acknowledgements
We thank Dr T. Kanesaki for helping with some experiments; Drs A. Spradling, E. Wieschaus, S. Roth, R. Karess, F. Matsuzaki, T. Isshiki, D. St Johnston and S. Hayashi for providing valuable materials; colleagues at NIG for suggestions and discussions; Drs S. Hayashi and E. Nakajima for critical reading of the manuscript; and the Kyoto Drosophila Stock Center, Bloomington Drosophila Stock Center, The Developmental Studies Hybridoma Bank, and The Drosophila Genomics Resource Center for providing fly strains, antibodies and DNA constructs.

Funding
This work was supported by a Grant-in-Aid for Science Research from the Ministry of Education, Science, Culture and Sports of Japan.

Competing interests statement
The authors declare no competing financial interests.

Author contributions
N.F. designed the study and analyzed the data. N.F. and F.Y. performed the experiments. N.F. and S.H. wrote the paper.

Supplementary material
Supplementary material available online at
http://dev.biologists.org/lookup/suppl/doi:10.1242/dev.093625/-/DC1

References
Barrett, K., Leptin, M. and Settleman, J. (1997). The Rho GTPase and a putative RhoGEF mediate a signaling pathway for the cell shape changes in Drosophila gastrulation. *Cell* **91**, 905-915.
Bosch, M., Serras, F., Martín-Blanco, E. and Baguñà, J. (2005). JNK signaling pathway required for wound healing in regenerating Drosophila wing imaginal discs. *Dev. Biol.* **280**, 73-86.
Brandman, O. and Meyer, T. (2008). Feedback loops shape cellular signals in space and time. *Science* **322**, 390-395.
Chen, C.-K., Burns, M. E., Spencer, M., Niemi, G. A., Chen, J., Hurley, J. B., Baylor, D. A. and Simon, M. I. (1999). Abnormal photoresponses and light-induced apoptosis in rods lacking rhodopsin kinase. *Proc. Natl. Acad. Sci. USA* **96**, 3718-3722.
Chen, Y., Li, S., Tong, C., Zhao, Y., Wang, B., Liu, Y., Jia, J. and Jiang, J. (2010). G protein-coupled receptor kinase 2 promotes high-level Hedgehog signaling by regulating the active state of Smo through kinase-dependent and kinase-independent mechanisms in Drosophila. *Genes Dev.* **24**, 2054-2067.
Cheng, S., Maier, D. and Hipfner, D. R. (2012). Drosophila G-protein-coupled receptor kinase 2 regulates cAMP-dependent Hedgehog signaling. *Development* **139**, 85-94.
Costa, M., Sweeton, D. and Wieschaus, E. (1993). Gastrulation in Drosophila: cellular mechanisms of morphogenetic movements. In *The Development of Drosophila melanogaster* (ed. M. Bate and A. Martinez Arias), pp. 425-465. New York, NY: Cold Spring Harbor Laboratory Press.
Costa, M., Wilson, E. T. and Wieschaus, E. (1994). A putative cell signal encoded by the folded gastrulation gene coordinates cell shape changes during Drosophila gastrulation. *Cell* **76**, 1075-1089.
Dawes-Hoang, R. E., Parmar, K. M., Christiansen, A. E., Phelps, C. B., Brand, A. H. and Wieschaus, E. F. (2005). folded gastrulation, cell shape change and the control of myosin localization. *Development* **132**, 4165-4178.
Fox, D. T. and Peifer, M. (2007). Abelson kinase (Abl) and RhoGEF2 regulate actin organization during cell constriction in Drosophila. *Development* **134**, 567-578.
Gelbart, M. A., He, B., Martin, A. C., Thiberge, S. Y., Wieschaus, E. F. and Kaschube, M. (2012). Volume conservation principle involved in cell lengthening and nucleus movement during tissue morphogenesis. *Proc. Natl. Acad. Sci. USA* **109**, 19298-19303.
Goltsev, Y., Fuse, N., Frasch, M., Zinzen, R. P., Lanzaro, G. and Levine, M. (2007). Evolution of the dorsal-ventral patterning network in the mosquito, Anopheles gambiae. *Development* **134**, 2415-2424.
Grishina, G. and Berlot, C. H. (1998). Mutations at the domain interface of GSalpha impair receptor-mediated activation by altering receptor and guanine nucleotide binding. *J. Biol. Chem.* **273**, 15053-15060.
Ikeshima-Kataoka, H., Skeath, J. B., Nabeshima, Y., Doe, C. Q. and Matsuzaki, F. (1997). Miranda directs Prospero to a daughter cell during Drosophila asymmetric divisions. *Nature* **390**, 625-629.
Jacinto, A., Wood, W., Balayo, T., Turmaine, M., Martinez-Arias, A. and Martin, P. (2000). Dynamic actin-based epithelial adhesion and cell matching during Drosophila dorsal closure. *Curr. Biol.* **10**, 1420-1426.
Jacinto, A., Woolner, S. and Martin, P. (2002). Dynamic analysis of dorsal closure in *Drosophila*: from genetics to cell biology. *Dev. Cell* **3**, 9-19.
Kanesaki, T., Hirose, S., Grosshans, J. and Fuse, N. (2013). Heterotrimeric G protein signaling governs the cortical stability during apical constriction in Drosophila gastrulation. *Mech. Dev.* **130**, 132-142.
Kato, K., Chihara, T. and Hayashi, S. (2004). Hedgehog and Decapentaplegic instruct polarized growth of cell extensions in the Drosophila trachea. *Development* **131**, 5253-5261.
Kiehart, D. P., Galbraith, C. G., Edwards, K. A., Rickoll, W. L. and Montague, R. A. (2000). Multiple forces contribute to cell sheet morphogenesis for dorsal closure in Drosophila. *J. Cell Biol.* **149**, 471-490.
Kölsch, V., Seher, T., Fernandez-Ballester, G. J., Serrano, L. and Leptin, M. (2007). Control of *Drosophila* gastrulation by apical localization of adherens junctions and RhoGEF2. *Science* **315**, 384-386.
Lecuit, T. and Lenne, P.-F. (2007). Cell surface mechanics and the control of cell shape, tissue patterns and morphogenesis. *Nat. Rev. Mol. Cell Biol.* **8**, 633-644.
Lee, S.-J., Xu, H. and Montell, C. (2004). Rhodopsin kinase activity modulates the amplitude of the visual response in Drosophila. *Proc. Natl. Acad. Sci. USA* **101**, 11874-11879.
Leptin, M. (2005). Gastrulation movements: the logic and the nuts and bolts. *Dev. Cell* **8**, 305-320.
Leptin, M. and Roth, S. (1994). Autonomy and non-autonomy in Drosophila mesoderm determination and morphogenesis. *Development* **120**, 853-859.
Martin, A. C. (2010). Pulsation and stabilization: contractile forces that underlie morphogenesis. *Dev. Biol.* **341**, 114-125.

Martin, A. C., Kaschube, M. and Wieschaus, E. F. (2009). Pulsed contractions of an actin-myosin network drive apical constriction. *Nature* **457**, 495-499.
Martin, A. C., Gelbart, M., Fernandez-Gonzalez, R., Kaschube, M. and Wieschaus, E. F. (2010). Integration of contractile forces during tissue invagination. *J. Cell Biol.* **188**, 735-749.
Molnar, C., Holguin, H., Mayor, F., Jr, Ruiz-Gomez, A. and de Celis, J. F. (2007). The G protein-coupled receptor regulatory kinase GPRK2 participates in Hedgehog signaling in Drosophila. *Proc. Natl. Acad. Sci. USA* **104**, 7963-7968.
Moore, C. A. C., Milano, S. K. and Benovic, J. L. (2007). Regulation of receptor trafficking by GRKs and arrestins. *Annu. Rev. Physiol.* **69**, 451-482.
Morize, P., Christiansen, A. E., Costa, M., Parks, S. and Wieschaus, E. (1998). Hyperactivation of the folded gastrulation pathway induces specific cell shape changes. *Development* **125**, 589-597.
Neer, E. J. (1995). Heterotrimeric G proteins: organizers of transmembrane signals. *Cell* **80**, 249-257.
Parks, S. and Wieschaus, E. (1991). The Drosophila gastrulation gene concertina encodes a G α-like protein. *Cell* **64**, 447-458.
Penn, R. B., Pronin, A. N. and Benovic, J. L. (2000). Regulation of G protein-coupled receptor kinases. *Trends Cardiovasc. Med.* **10**, 81-89.
Pitcher, J. A., Freedman, N. J. and Lefkowitz, R. J. (1998). G protein-coupled receptor kinases. *Annu. Rev. Biochem.* **67**, 653-692.
Ratnaparkhi, A. and Zinn, K. (2007). The secreted cell signal Folded Gastrulation regulates glial morphogenesis and axon guidance in Drosophila. *Dev. Biol.* **308**, 158-168.
Rogers, S. L., Wiedemann, U., Häcker, U., Turck, C. and Vale, R. D. (2004). Drosophila RhoGEF2 associates with microtubule plus ends in an EB1-dependent manner. *Curr. Biol.* **14**, 1827-1833.
Ross, E. M. (2008). Coordinating speed and amplitude in G-protein signaling. *Curr. Biol.* **18**, R777-R783.
Roth, S. (2004). Gastrulation in other insects. In *Gastrulation: From Cell to Embryo* (ed. C. D. Stern), pp. 105-121. New York, NY: Cold Spring Harbor Laboratory Press.
Roth, S., Stein, D. and Nüsslein-Volhard, C. (1989). A gradient of nuclear localization of the dorsal protein determines dorsoventral pattern in the Drosophila embryo. *Cell* **59**, 1189-1202.
Royou, A., Sullivan, W. and Karess, R. (2002). Cortical recruitment of nonmuscle myosin II in early syncytial *Drosophila* embryos: its role in nuclear axial expansion and its regulation by Cdc2 activity. *J. Cell Biol.* **158**, 127-137.
Sánchez-Madrid, F. and del Pozo, M. A. (1999). Leukocyte polarization in cell migration and immune interactions. *EMBO J.* **18**, 501-511.
Schneider, L. E. and Spradling, A. C. (1997). The Drosophila G-protein-coupled receptor kinase homologue Gprk2 is required for egg morphogenesis. *Development* **124**, 2591-2602.
Solnica-Krezel, L. and Sepich, D. S. (2012). Gastrulation: making and shaping germ layers. *Annu. Rev. Cell Dev. Biol.* **28**, 687-717.
Sweeton, D., Parks, S., Costa, M. and Wieschaus, E. (1991). Gastrulation in Drosophila: the formation of the ventral furrow and posterior midgut invaginations. *Development* **112**, 775-789.
Tall, G. G., Krumins, A. M. and Gilman, A. G. (2003). Mammalian Ric-8A (synembryn) is a heterotrimeric Galpha protein guanine nucleotide exchange factor. *J. Biol. Chem.* **278**, 8356-8362.
Tanoue, S., Krishnan, P., Chatterjee, A. and Hardin, P. E. (2008). G protein-coupled receptor kinase 2 is required for rhythmic olfactory responses in Drosophila. *Curr. Biol.* **18**, 787-794.
Turner, F. R. and Mahowald, A. P. (1977). Scanning electron microscopy of Drosophila melanogaster embryogenesis. II. Gastrulation and segmentation. *Dev. Biol.* **57**, 403-416.

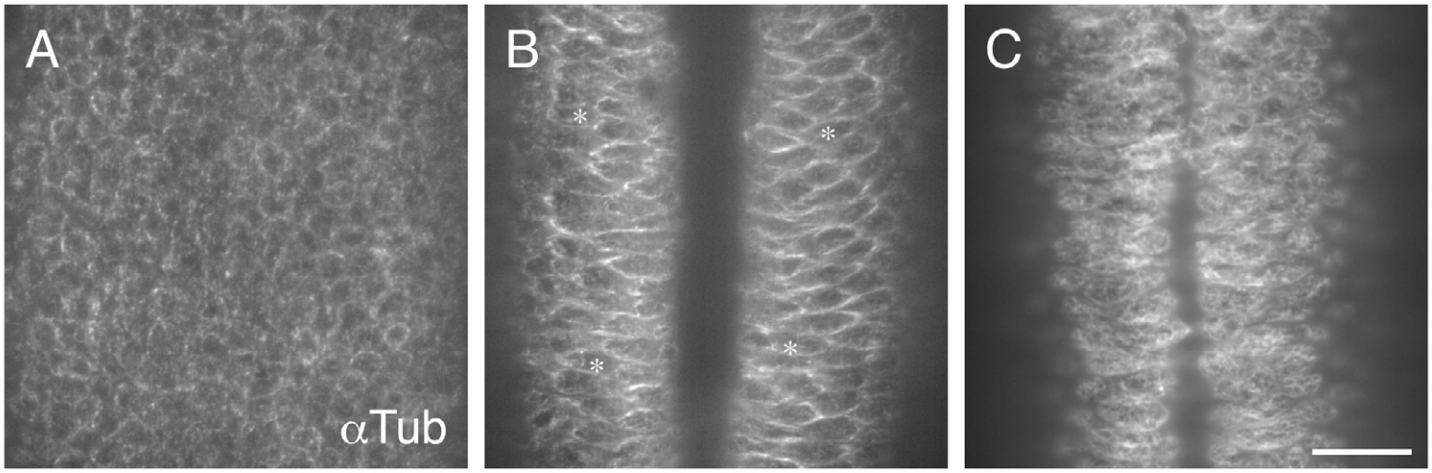

Fig. S1 Immuno-staining for α-Tubulin
Wild-type embryos before gastrulation (A), and at middle (B), and late (C) stages of gastrulation were stained for α-Tubulin. The focus was adjusted on the ventral surface of embryos. Some LM cells bearing a thin protruding structure (likely corresponding to an apical protrusion) are marked with asterisks. These thin structures were observed at the middle stage of gastrulation. Scale bar: 20μm.

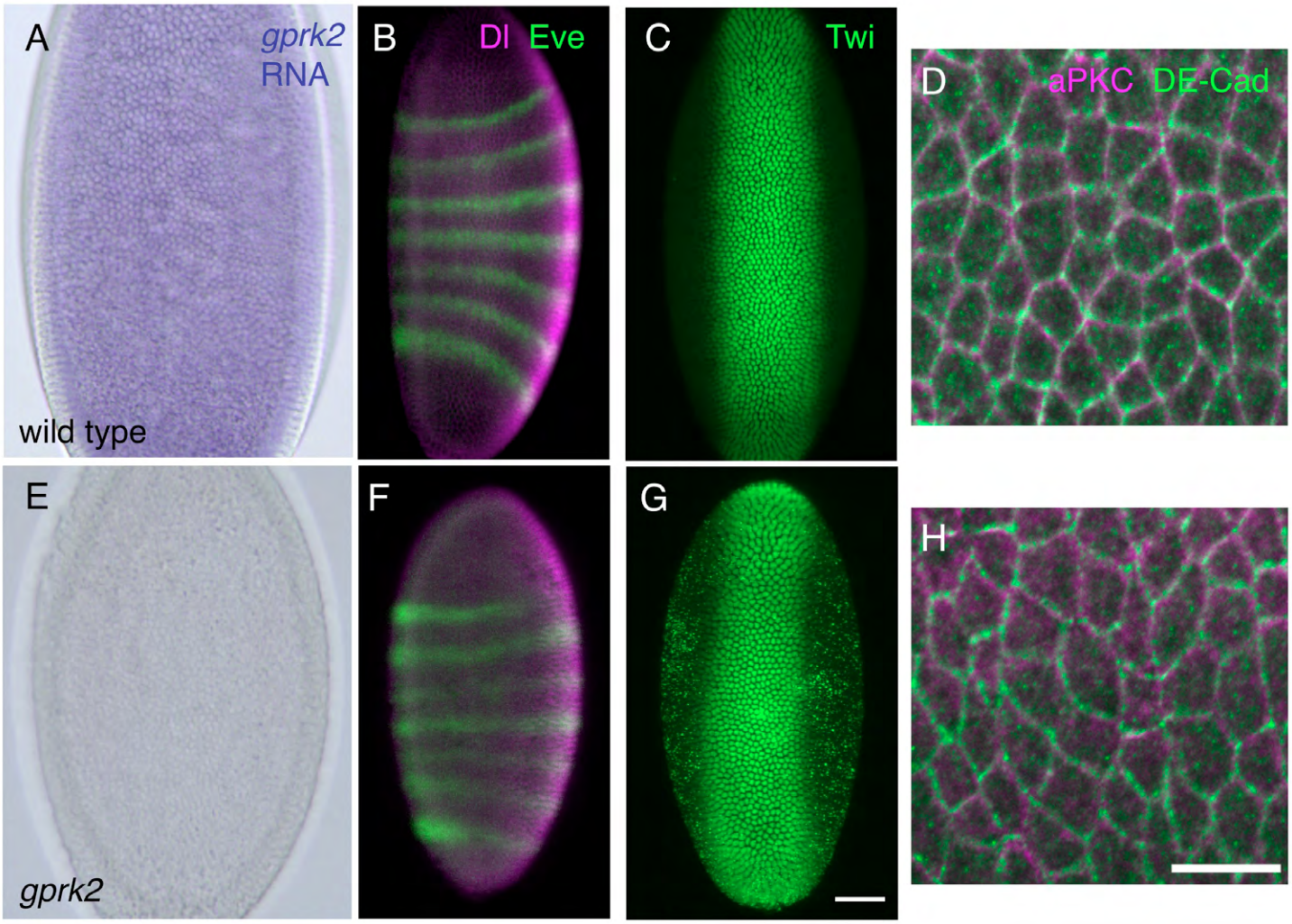

Fig. S2 Axial patterning and adherence junction in *Gprk2* mutant embryos
Wild-type embryos (A-D) and *Gprk2* mutant embryos (E-H) stained for *Gprk2* RNA (A, E), for Dl and Eve proteins (B, F), for Twi protein (C, G) and for aPKC and DE-Cadherin proteins (D, H). *Gprk2* RNA is expressed uniformly in wild-type embryos, but is not expressed in *Gprk2* mutant embryos (A, E). Ventral views (A, C, E, G) and lateral views (B, F) are shown. The staining of scattered particles in G is non-specific background. High-magnification views of lateral ectodermal cells focused on the sub-apical section indicate cortical localization of aPKC and DE-Cadherin (D, H: anterior is toward left). Scale bars: (G) 50 μm, (H) 20 μm.

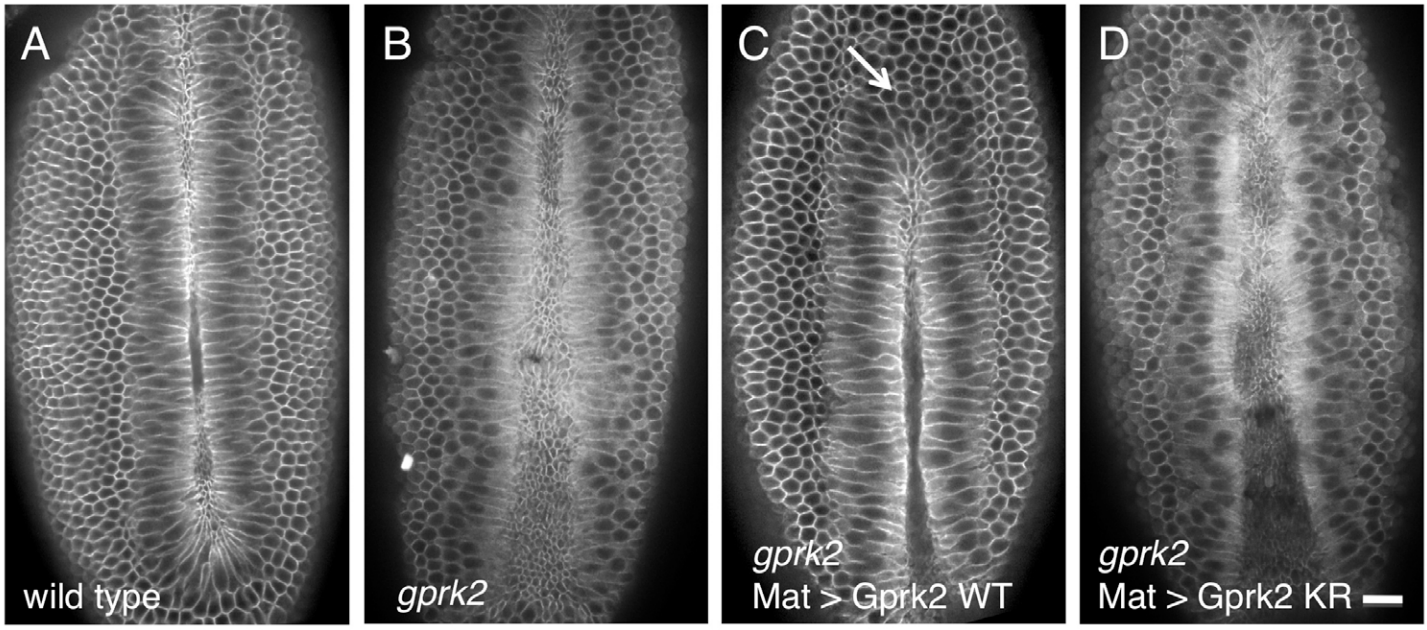

Fig. S3 Rescue experiment for *Gprk2* mutant
(A) Wild-type embryo, (B) *Gprk2* mutant embryo, (C) *Gprk2* mutant embryo with Maternal-Gal4-driven Gprk2 (wild-type) expression, (D) *Gprk2* mutant embryo with Maternal-Gal4-driven Gprk2 (K338R) expression. Embryos were stained for Dlg protein. (C) The wild-type Gprk2 transgene partially blocked apical constriction (arrow). Scale bar: 20 μm.

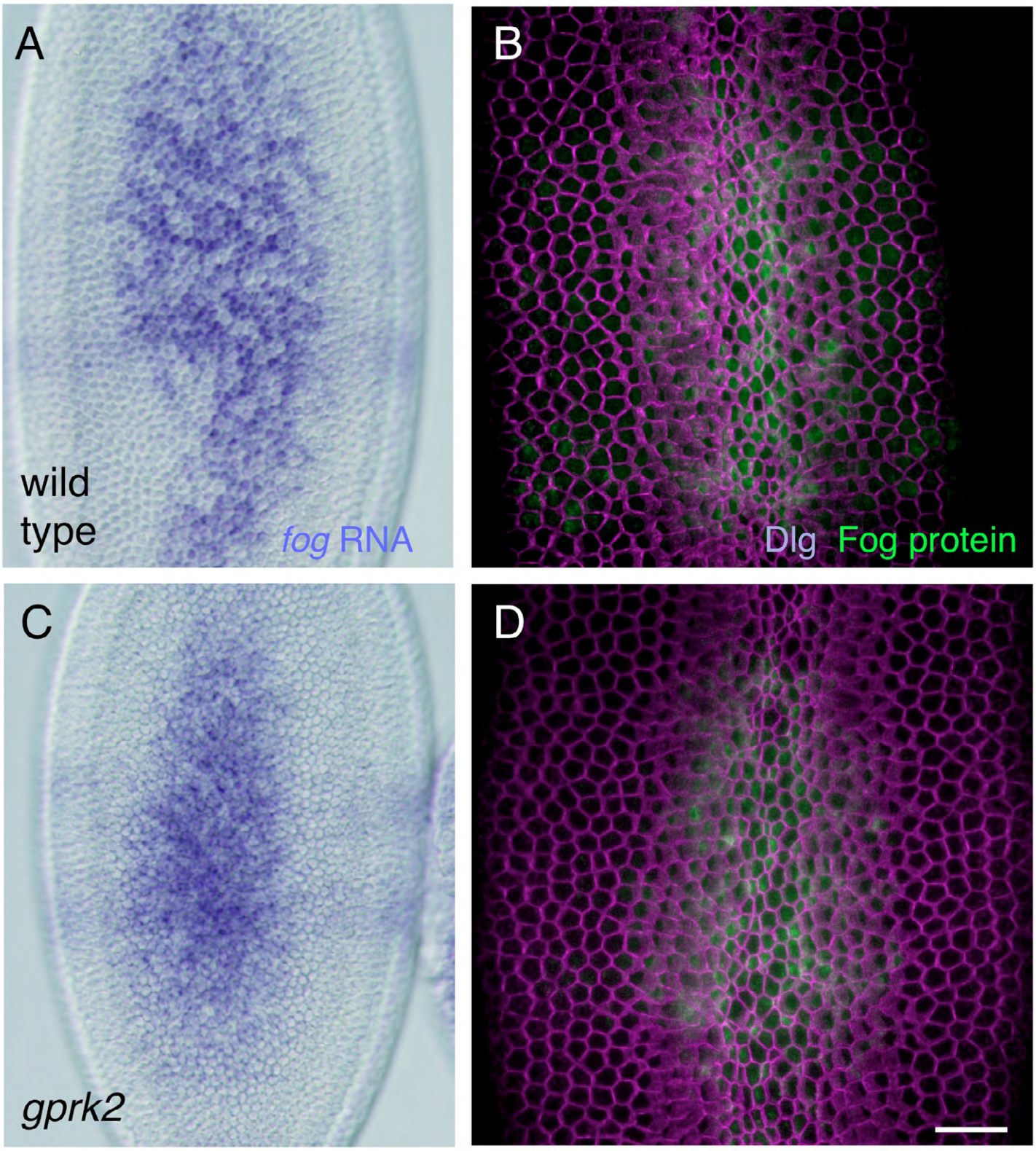

Fig. S4 Fog expression in *Gprk2* mutant embryos
(A, C) *fog* RNA expression was detected by Dig-AP staining in wild-type (A) and *Grpk2* mutant (C) embryos. (B, D) Wild-type (B) and *Gprk2* mutant (D) embryos were stained for Dlg and Fog proteins. Fog protein is expressed in a similar pattern in wild-type (B) and *Gprk2* mutant (D). Scale bar: 20 μm.

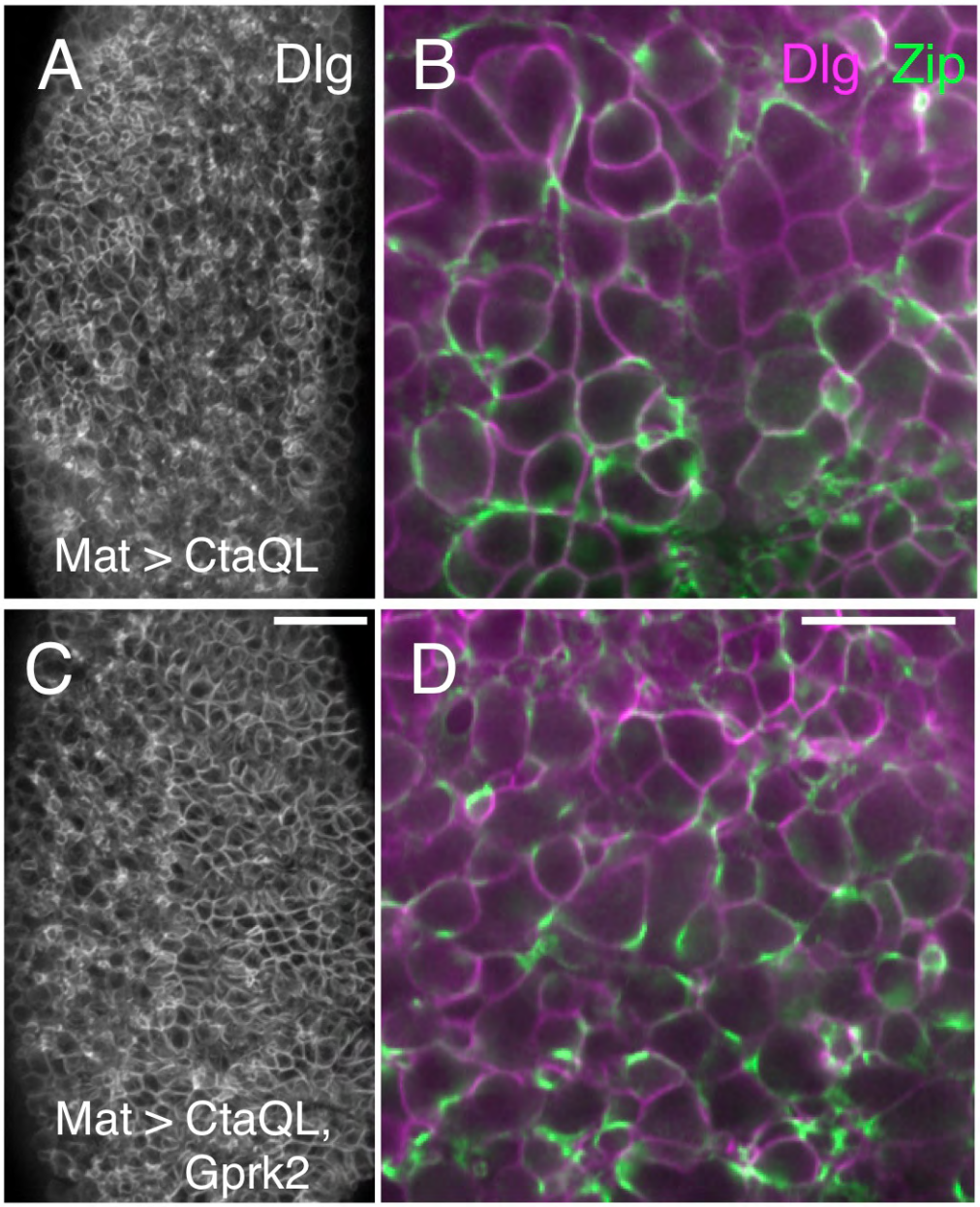

Fig. S5 Over-expression of Cta Q303L and Gprk2
(A, C) Embryos at late gastrulation stage were stained for Dlg protein. (B, D) High-magnification views of the apical surface of lateral ectodermal cells stained for Dlg and Zip proteins. Anterior is toward left and dorsal is toward the top. Genotypes of the embryos were Maternal-Gal4, UAS-Cta Q303L (A, B), and Maternal-Gal4, UAS-Cta Q303L, UAS-Gprk2 (C, D). Scale bars: (C) 20 μm, (D) 10 μm.

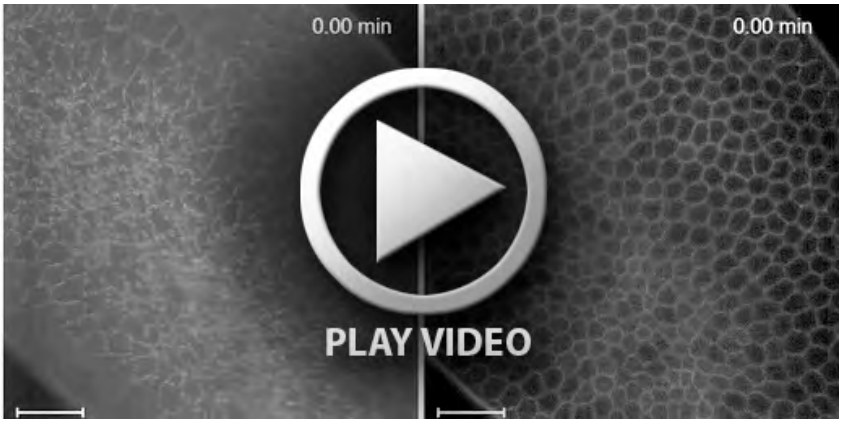

Movie 1 Time-lapse movie of apical surface of gastrulae
Movie of ventral view of a living Moe::GFP embryo. Focus was adjusted on the surface (left) and 9 μm depth (right) of the same embryo. Time 0 was taken at the start of observation. Anterior is toward the upper left.

Movie 2 Dynamics of apical protrusions
High magnification views of Movie 1. Focus was adjusted on the surface (left) and 9 μm depth (right) of the same area. While LM cells moved toward mid-ventral (the lower left), apical protrusions dynamically changed their morphology.

Movie 3 Analysis of cell movements
An example of tracking of cell movements of a Moe::GFP embryo. Focus was adjusted at 7 μm depth. Anterior is toward the upper left. The cell vertexes chosen for tracking are marked with colored circles.

Movie 4 Time-lapse movie of Moe::GFP embryo
Movie of ventral view of a living Moe::GFP embryo. Five stacked images along the Z-axis (4 μm depth) were merged by maximum intensity projection. Anterior is toward the top.

Movie 5 Time-lapse movie of *gprk2* mutant embryo with Moe::GFP
Movie of ventral views of a living *gprk2* mutant embryo with Moe::GFP. Five stacked images along the Z-axis (4 μm depth) were merged by maximum intensity projection. Anterior is toward the bottom. Images of Fig. 4C were rotated 180°.

Movie 6 Time-lapse movie of Sqh::GFP embryo
Movie of ventral view of a living *gprk2* heterozygote embryo with Sqh::GFP as a control. Ten stacked images along the Z-axis (9 μm depth) were merged by maximum intensity projection. Anterior is toward the top.

Movie 7 Time-lapse movie of *gprk2* mutant embryo with Sqh::GFP
Movie of ventral views of a living *gprk2* homozygote mutant embryo with Sqh::GFP. Ten stacked images along the Z-axis (9 μm depth) were merged by maximum intensity projection. Anterior is toward the top.